Geomorphology 450 (2024) 109069

Contents lists available at ScienceDirect

Geomorphology

journal homepage: www.journals.elsevier.com/geomorphology

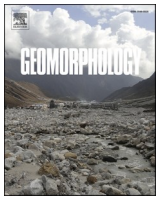

Spatio-temporal analysis of geomorphic recovery along an altered ephemeral stream using automated image processing

Maria Pilar Rabanaque [a,*], Vanesa Martínez-Fernández [b], Mikel Calle [c,d], Olegario Castillo [e], Gerardo Benito [a]

[a] Departamento de Geología, Museo Nacional de Ciencias Naturales – CSIC, Calle Serrano 115 bis, 28006 Madrid, Spain
[b] Departamento de Sistemas y Recursos Naturales, E.T.S. Ingeniería de Montes, Forestal y del Medio Natural, Universidad Politécnica de Madrid, Spain
[c] Geography and Geology Department, University of Turku, Turku, Finland
[d] Turku Collegium for Science, Medicine and Technology, Turku, Finland
[e] Departamento de Ingeniería Industrial e Ingeniería Civil, Escuela Técnica Superior de Ingeniería de Algeciras, Universidad de Cádiz, 11202 Algeciras, Cádiz, Spain

ARTICLE INFO

Keywords:
River recovery
Gravel mining
Ephemeral river
Sediment connectivity
Machine learning
Automatic segmentation

ABSTRACT

Ephemeral rivers in the Mediterranean region have been exposed to significant human disturbance over the last century. Recently, there has been a growing interest in restoring their morpho-sedimentary condition, backed by the European Water Framework Directive. Previous research has highlighted the severe geomorphic impacts of sediment extraction, such as reduced channel width and riverbed incision, but the recovery of these channels during annual flows remains poorly understood. This study presents a methodological framework to investigate geomorphologic recovery (signs of landform change) and constraints in the Rambla de Cervera (eastern Spain) from 2018 to 2021. Aerial imagery, LiDAR topography, and field surveys were used for stream segmentation, fluvial landform classification, temporal landform change, and comparison with flow characteristics from a 2D hydraulic model. The study identified three groups of segments with different channel types and recovery mechanisms. Upstream (G1), unconfined valley settings showed minor changes, indicating morphological stability. Middle segments in confined valleys (G2) showed greater alluvial channel recovery and vegetation encroachment in response to flood/no-flood periods. Downstream segments (G3), incised on cemented gravel, were highly responsive to floods but lacked landform stability due to high energy conditions. The findings suggest that channel recovery during annual floods is slow and occurs mainly downstream in degraded areas (G3). Increased sediment flux from upstream and additional sediment storage in new forms are required to recover these channels. This analysis underscores the challenge of interpreting short-term morpho-dynamic changes for long-term river recovery, but provides insight into the morpho-sedimentary conditions required to accelerate recovery of ephemeral streams.

1. Introduction

Over the past 80 years, Mediterranean ephemeral rivers have been extensively altered by intensive human actions such as gravel mining (Kondolf, 1997; Batalla, 2003; Calle et al., 2020), dam construction (Batalla et al., 2006; Segura-Beltrán and Sanchis-Ibor, 2013), linear infrastructures (e.g., road traffic, conduits) (Ollero et al., 2022), reforestation, dumping of trash and irrigation schemes (Suárez and Vidal-Abarca, 2008). These anthropogenic activities have interrupted sediment-water nutrient fluxes leading to significant morphodynamic changes (Rinaldi, 2003; Sanchis-Ibor et al., 2017). Although ephemeral rivers are governed by the same hydraulic and geomorphological processes as perennial rivers, the spatio-temporal variability of their discharge and the lack of a base flow for most of the year make them especially vulnerable to any environmental pressures (Ollero et al., 2022). Among others, the incision of the channel bed (Segura-Beltrán and Sanchis-Ibor, 2013), the lack of longitudinal sedimentary connection (Calle et al., 2017), the armouring of the bed and the increase of vegetated bars, strongly related to the decrease in morphological activity (Picco et al., 2023), are the main elements for the diagnosis of degradation. The lack of adequate environmental legislation, the development of economic activities (tourism, agriculture, etc.), and the

* Corresponding author.
E-mail address: m.rabanaque@mncn.csic.es (M.P. Rabanaque).

https://doi.org/10.1016/j.geomorph.2024.109069
Received 20 September 2023; Received in revised form 15 January 2024; Accepted 15 January 2024
Available online 22 January 2024

weak social dimension regarding environmental issues contributed to the existing ecological and morpho-sedimentary fluvial degradation. After decades of abandonment, there is growing interest in fluvial recovery of morpho-sedimentary and ecological conditions, legislated in Europe by the Water Framework Directive (WFD; (European Commission, 2000)). The WFD requires water bodies to reach a hydromorphological condition capable of supporting a good ecological status (cf Newson and Large, 2006). Recent scientific initiatives made significant efforts to adapt the WFD to intermittent rivers and ephemeral streams (Datry et al., 2017; Gallart et al., 2017). These advances were focussed on new ecohydrological indicators based on plant habitat, aquatic species and the physico-chemical quality of the water from samplings carried out during the flow runs or in pools that may persist during the dry season (Gallart et al., 2017; Stubbington et al., 2019). However, the implementation of classical water quality indicators in ephemeral streams is still challenging given the shortness of flow events and the limited timing of water in pools. Therefore, it is critical that morpho-sedimentary criteria take relevance, providing new tools integrating hydrology, geomorphology and riparian ecology in the assessment of the environmental status and geomorphological recovery from disturbance of Mediterranean streams (e.g., Piégay et al., 2016). In particular, in degraded ephemeral streams recovery criteria need to quantify fluvial dynamics and landform heterogeneity in response to hydrological events. Critically, the high degree of adjustment of ephemeral rivers to the occasional high magnitude flood events has been demonstrated (Hooke, 2016a). Therefore, a systematic understanding of the effects of extreme and annual flow events on recovery trajectories requires new semi-automated methods to determine event-related changes in morphological heterogeneity and their links to hydrological processes.

The analysis of the geomorphic recovery of rivers is based on an assessment of the geomorphic status and on a deep understanding of the catchment-wide variability in river morphology and processes (see Fryirs and Brierley, 2016; Horacio et al., 2017). Geomorphic assessments typically include a historically informed analysis of changes over time and a contemporary survey evaluation of factors such as hydrology, longitudinal connectivity and transversal structure (i.e., vegetation-landforms interactions, valley corridor and alluvial-bedrock channel structure). The historical evolution analysis is supported by aerial photographs and allows us to determine what accommodation space, activation processes and establishment of landform sequences are required to recover some degree of equilibrium state (Fuller et al., 2021; Rabanaque et al., 2021). This long-term perspective also informs about the maximum margins of recovery that can occur under natural conditions (Rinaldi et al., 2016). Then, the geomorphic sensitivity to change understood as the likelihood that a given change in the controls of a system will produce a meaningful, discernible and persistent response (Brunsden and Thornes, 1979), can then be explored through channel recovery (evidence of landform change) and channel stabilisation by vegetation colonisation. It is worth noting that many historical changes are irreversible, so that the pre-disturbance condition is no longer a realistic target condition for recovery and restoration actions (Dufour and Piégay, 2009).

Recent river recovery efforts have also emphasised identification of the primary causes of morphodynamic and ecological degradation and the description of adjustment processes (e.g., Kondolf et al., 2006). Restoration thus focusses on reestablishing normative rates and magnitudes of physical, chemical, and biological processes responsible for floodplain and channel formation and maintenance (Beechie et al., 2010). The potential for river recovery depends on (1) the spatial configuration of the state variables (valley shape and landform units) and (2) the system dynamics and processes (water-sediment-nutrient fluxes) in response to forcing factors (magnitude-frequency of flow events). These system variables are often described as physical (structural) and dynamic (process-based) boundary conditions (constraints) within which rivers adjust over time (e.g., Mould and Fryirs, 2018). This approach introduces the complexity that various drivers that influence the magnitude and rate of channel change (e.g., sediment load, storage, transport) are unevenly distributed across the catchment, and therefore, there is potential for reach-differentiated channel morphodynamics (Downs et al., 2013). This reach-scale differentiation reflects the spatio-temporal variability of geomorphic controls and processes determining the rate and trajectory of channel recovery (Brierley and Fryirs, 2016; Mould and Fryirs, 2018). Therefore, a reach-scale analysis, identifying physical and process constraints, is central to understanding channel response to multiple drivers (Downs et al., 2013).

Detailed geomorphological data with relatively high spatial and temporal resolution are required to understand the morphodynamic response and recovery evolution (Bizzi and Lerner, 2012; Carbonneau et al., 2020). In most cases, repeated geomorphological data are often expensive and time-consuming, so their availability is often a problem. New image processing techniques and recent applications to very high resolution (0.25 m) aerial orthophotographs provide a rich source of data to accurately track change in landform change over time accurately and to assess the impact of natural and human-induced processes on the environment. Such data can be collected by remote sensing, aerial photography and field mapping at annual or sub-annual time scales and cover the entire watershed at reach scale (Rabanaque et al., 2021). In addition, the automated image processing combined with statistical tools to spatially segment the fluvial system (Martínez-Fernández et al., 2016) becomes a powerful tool to assist and focus future management decisions on river conservation and restoration.

Herein we present a multiscale spatial framework with a multi-temporal analysis to assess short-term channel recovery in response to flood events. This method allows the identification of models of channel morphodynamics, critical reaches that inhibit sediment flux and recovery, and potential actions to accelerate the geomorphological integrity of highly altered ephemeral rivers. This framework is exemplified in an ephemeral river that has been subject to a regionally typical pattern of instream gravel extraction since the 1970s, a regionally extended practice that makes this case study representative of most of the Mediterranean ephemeral streams.

2. Study area and regional settings

The Rambla de Cervera is a 44 km long ephemeral stream draining into the Mediterranean Sea, in eastern Spain. It drains a catchment area of ~340 km^2 with a maximum elevation of 1160 m.a.s.l. and an average slope of 1.4 % (Sanchis-Ibor and Segura-Beltrán, 2014). The Rambla de Cervera catchment comprises two main geological domains, the Iberian chain (the headwaters), and the Maestrat graben system (the middle and lower reaches). The study area lies within the graben and horst structures (Fig. 1), whose configuration is the result of an extensional tectonic event, initiated in the late Oligocene to early Miocene, which fractured the Mesozoic calcareous rocks of the Iberian Chain (Simón et al., 2013). This resulted in a series of small basins that were filled with alluvial deposits and lacustrine sediments (Anadón and Moissenet, 1996). Subsequent activation of the tectonic fractures developed the current configuration of the river network (Simón et al., 2013), which crosses several of these horst and graben sequences. This creates narrow gorges and wide valleys with alternating conditions of limited sediment supply or higher sediment availability.

The climate of the Rambla de Cervera is Mediterranean, with an average annual temperature of 9 °C degrees in the headwaters and 15 °C near the sea. Average rainfall is 700 mm in the highlands and 480 mm in the lowlands. Maximum rainfall occurs in spring and autumn, with summer being the driest season. Streamflow episodes occur mainly associated with heavy rainfall (>50 mm accumulated), on average two to four times a year (Sanchis-Ibor and Segura-Beltrán, 2014).

The main changes in land use at the watershed scale from the 1950s to the present are related to the abandonment of agricultural land due to a crisis of the traditional dry farming and the migration of people to the

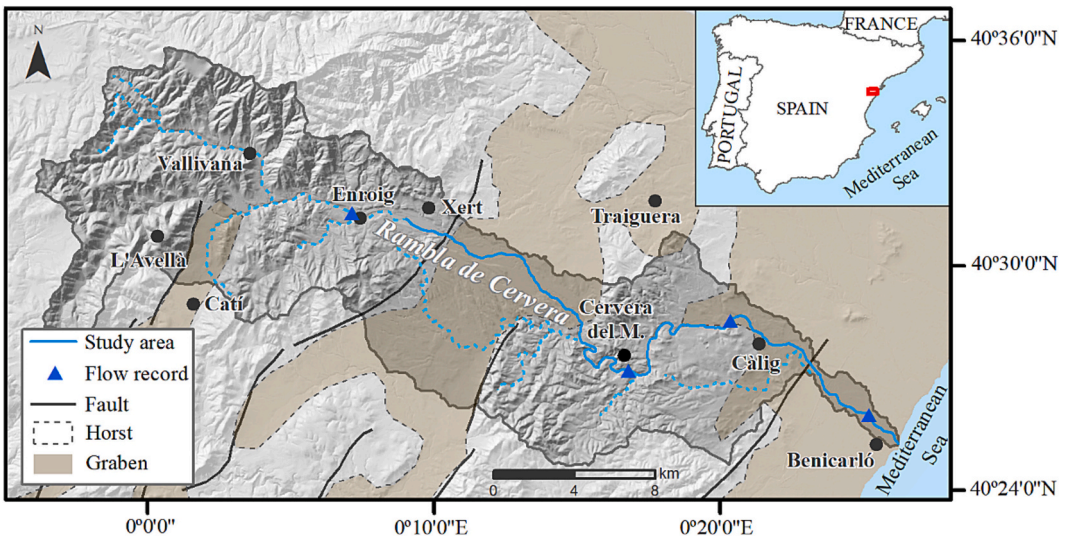

Fig. 1. The Rambla de Cervera catchment and location of the main structural features conditioning the width of the valley corridor. The study area comprises between Xert and Benicarló at the junction with the Mediterranean Sea. Inset: The Iberian Peninsula showing the location of the Rambla in eastern Spain.

cities mainly between 1950 and 1970 (Segura-Beltrán and Sanchis-Ibor, 2013). These abandonments favoured the growth of natural or reforested forests which reduced direct runoff in the watershed. The extraction of gravel directly from the river channels was intensive from the 1970s to the 2000s with similar intensity along the studied reach. This extraction was not regulated and the volume extracted between 1980 and 2007 is estimated to be close to 358,040 m^3. The peak of extraction was between 1980 and 1988, with an average of 36,600 m^3/year (Segura-Beltrán and Sanchis-Ibor, 2013). After these years, gravel mining gradually declined and the authorities began to regulate it in order to reduce its impact. However, some extraction sites are still active today, and this, together with the effects of past activities, strongly influences current sediment availability and river morphodynamics.

These gravel extractions have led to significant changes in this ephemeral stream from braided to a wandering pattern, with a continuous reduction in channel width of ~68.5 % between Enroig and Cervera del Maestre, most pronounced in the period 1946–1956 (Segura-Beltrán and Sanchis-Ibor, 2013). This was accompanied by a 3–4 m incision, mainly after 1977 (Segura-Beltrán et al., 2020), which was more pronounced downstream of Càlig. These geomorphic changes,

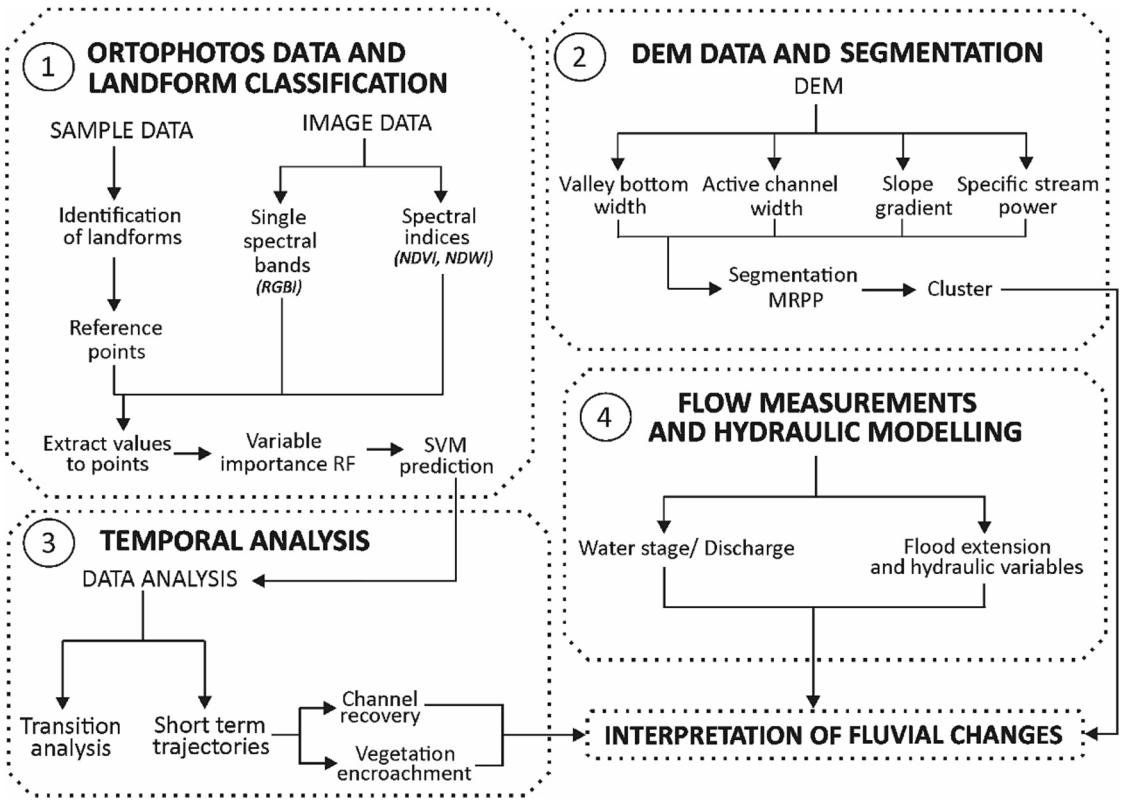

Fig. 2. General workflow diagram used in this work. RF: random forest; SVM: support vector machine; DEM: digital elevation model; MRPP: multi-response permutation procedure.

particularly in relation to channel confinement, have significantly altered the physical characteristics of the channel, namely its shape, gradient, topography, bed texture and bank materials.

3. Methods

The research methods and workflow used in this paper are divided into four steps (Fig. 2): (1) pre-processing of orthophoto data (i.e., calculation of spectral indices) and manual collection of landform sample data to perform a supervised classification; (2) extraction of geomorphic variables and multivariate segmentation; (3) temporal analysis of the supervised classification results by estimating changes in landform classes on a yearly basis; (4) hydrological characterization and hydraulic modelling of the flow events during the study period.

3.1. Classification of fluvial landforms

3.1.1. Sampling for supervised classification and estimation of spectral indices

To develop the fluvial landform analysis, we identified four distinct classes based on surface cover following Sanchis-Ibor et al. (2017) and Rabanaque et al. (2022): i) bedrock; ii) bare sediment scarcely covered by grasses and scattered shrubs (<5 % of vegetation); iii) mixed vegetated areas, covered by shrubs (<50 %) and scattered trees (<5 %); iv) dense mature areas, covered by dense patches of woody vegetation and trees (>50 %) in alluvial areas. These classes were visually identified by using very high resolution RGB aerial orthophotos (0.25 m/pixel) from the Institut Cartogràfic Valencià (www.icv.gva.es). These orthophotos are available annually for the study period (2018–2021) and include near-infrared bands in addition to RGB. The number of pixel sample points also varies, given that the acquisition period is between May and August. In some categories, the sample points are the same, while in 2020 and 2021 the category bare sediment had to be strengthened (Table 1) due to the high brightness of the images.

3.1.2. Supervised classification of river landforms using SVM algorithm

RGBI bands and spectral indices (i.e., NDVI (Rouse et al., 1974), NDWI (McFeeters, 1996) and, Coloration Index (CI, Escadafal and Huete, 1991)) were used to calculate the importance of variables in order to optimise the supervised classification of surface and reduce the time consuming and computationally intensive process. This process was performed using Random Forest (RF), a machine learning algorithm based on tree decision rules (Breiman, 2001). We used the Gini impurity index in this algorithm to determine the importance of these variables, which was replicated 30 times to obtain a consistent measure of the impurity of each variable by k-fold cross-validation (k = 3) and repeated 10 times. The original sample data was divided into 3 sets, two of which were used for training (66 %) and one for validation (33 %). RF, like any other machine learning algorithm, requires an optimisation of the hyperparameters in order to use the best ones for variable selection. In this case, the optimisation was obtained after 10-fold repeated cross-validation, with a number of 1–5 random predictors selected in each decision tree (*mtry*), a minimum size of a node to be split (*min.node.size*) of 2–30 and with a value of 500 in the number of trees (*ntree*). This process was performed using the "*caret*" package (Kuhn, 2020) in the R program (R Core Team, 2022).

Once the results of the best variables for each year were obtained, a supervised classification of the entire river surface was performed using the Support Vector Machine (SVM) algorithm (Cortes and Vapnik, 1995). This is one of the best techniques for modelling changes in land use or land cover (Phiri et al., 2020). The SVM consists of separating the different categories on a hyperplane as well as possible (Cortes and Vapnik, 1995). To do this, the sample points were divided into 80 % for training the model and 20 % for validation, and then the hyperparameters were optimised. The hyperparameters are gamma and cost. Gamma specifies the influence of each training example, while cost maximises the range of the decision function by compensating for the correct classification of the training examples. Gamma ranges from 0.001 to 1, while cost ranges from 1 to 700. For land use classification, the radial kernel is used due to its good performance (Thanh Noi and Kappas, 2018). Once the classifications were obtained, the results were verified. In some areas, the bedrock class was confused with bare sediment and was manually corrected using the "Pixel Editor" tool in ArcGIS Pro.

Table 1
Acquisition date and number of sample points for each landform.

Year	2018	2019	2020	2021
Acquisition date	13/06/2018–24/08/2018	14/05/2019–30/06/2019	02/05/2020–31/05/2020	13/05/2021–15/08/2021
Number of sample points per class				
Bedrock	107	107	107	107
Bare sediment	114	114	122	122
Dense mature areas	132	132	132	132
Mixed vegetated areas	130	130	130	130
Total	483	483	491	491

3.2. Geomorphic variables and river segmentation

In order to study the temporal evolution of the river response as a function of the geomorphical characteristics of the river reaches, we used an automated multivariate procedure to establish internally homogeneous river segments. These objective methods allow the discretisation of the river system based on statistical criteria (Alber and Piégay, 2011; Martínez-Fernández et al., 2016). In this process, multivariate methods allow the consideration of complementary information provided by several variables to be taken into account (Bizzi and Lerner, 2012; Martínez-Fernández et al., 2019).

In this case, four geomorphic variables were used to characterise and segment the Rambla de Cervera: (1) valley bottom width, (2) active channel width, (3) slope gradient and, (4) specific stream power. The four variables were extracted from a 2 m resolution DEM of the latest Spanish National Plan for Aerial Orthophotography Lidar Project (PNOA-LiDAR Project) at 200 m intervals along the valley axis in a GIS environment (Martínez-Fernández et al., 2016) using FluvialCorridor 10.5 (Roux et al., 2015).

The width of the valley bottom (VBW) was automatically obtained from the DEM using FluvialCorridor 10.5 (Roux et al., 2015) divided by 200 m. The active channel was obtained from the most recent orthophoto (i.e., 2021) and it was digitized manually by identifying the areas covered by bare sediment and bedrock, although some vegetation patches could be included inside this polygon. This implies that some areas were occupied by mixed vegetated areas or dense mature areas in 2018. Mean active channel width (ACW) was obtained as the active channel area in the most recent year divided by the reach length (i.e., 200 m). For each division, the slope gradient (SG) was calculated as the difference in elevation between the point 200 m upstream and the point 200 m downstream, divided by the total distance (i.e., 400 m). Finally, the specific stream power (SSP) or stream power (ω) per unit width was calculated, as follows: $\omega = \gamma Qs/w$ where γ is the specific weight of water (9800 N/m^3), *Q* is the water discharge, s is the energy slope (m/m) and *w* is the width (Knighton, 1999). The discharge value (Q) was obtained from the 'CAUMAX' (CEDEX, 2013) dataset associated with a 2-year flow event, and the width (w) was set to the active channel width obtained from the 2021 orthophoto delineation.

Multi-response permutation procedures (MRPP, Mielke, 1991) were then used to perform the river segmentation using R (R Core Team, 2022). The four variables were previously standardised and an alpha

risk of 0.05 was considered to be statistically significant. Further details of the procedure can be found in Martínez-Fernández et al. (2016).

3.3. Temporal analysis of river response

Monitoring morphological change following anthropogenic disturbance requires a temporal perspective to determine morphological adaptation and thresholds of response to flows of different magnitudes. In this way, pathways of river recovery and resilience to human disturbance and flow regimes can be identified. Spatio-temporal changes of the four classes based on surface cover (i.e., bedrock; bare sediment with scarce vegetation cover; mixed vegetated areas with shrubs and scattered trees; and dense mature areas) were mapped from orthophotos taken annually between 2018 and 2021 (see Section 3.1). Therefore, an interannual transition analysis was used to quantify the proportion of change between surface classes, providing relevant information on the stability and/or dynamics of the fluvial system. Those surfaces that evolve towards more active surfaces are considered to be channel recovery transitions, e.g., those surfaces that change from vegetated areas, whether mixed or dense vegetated areas, to bare gravel bars. Conversely, those areas that have been stabilised by vegetation colonisation and are partially or completely covered by vegetation are considered as vegetation encroachment transitions. These transitions are analysed by calculating the proportion of change between consecutive years, but also calculating the net proportion of change between 2018 and 2021, and visualised by drawing chord diagrams using the "*circlize*" package (Gu, 2022) in R Studio (R Core Team, 2022). These graphs allow seeing the changes between the classes.

3.4. Flow characterization of the study period

Surface water levels were monitored at four sites along the Rambla (Enroig, Cervera del Maestre, Càlig and Benicarló, Fig. 1) using submersible pressure transducers (Levelogger® model 3001 by Solinst). These pressure transducers recorded the combined atmospheric pressure and the pressure exerted by the overlying water column. The data were corrected using the nearby barometric pressure transducer. Measurements were taken at 5 minute intervals. A level concrete road crossing the streambed was used as the location for the water level gauges (Fig. 3). High-water marks (HWMs) were measured at the gauging sites after each flood event. The gauged records and HWMs were used for the calibration of the 2D hydraulic model, namely the IBER software (Bladé et al., 2014). This model solves the 2D Saint Venant equations using explicit finite volume schemes on a triangulated mesh obtained directly from a digital terrain model (DTM). The DTMs were obtained from the LiDAR data collected by the PNOA project in 2017. In addition, field surveys were carried out in the field, namely on the road surface, using differential GPS. In the case of the Benicarló site, the bridge piers were modelled in ArcGIS to fill the LiDAR data gap under the bridge. The hydraulic model was used to derive the rating curve and estimate the hydrograph and peak discharge of each event. The flows were routed to calculate the flow characteristics and hydraulic parameters (unit stream power, shear stress and discharge) along the study area.

4. Results

4.1. Classification and segmentation outcomes

The order of importance of the variables in the image classification varied from year to year. For all the years, we selected the variables that were higher than 70 % of the median for the SVM models. These variables were CI and NDVI in 2018, NDWI and CI in 2019, NDVI and NDWI for 2020 and, NDWI and NDVI in 2021 (Fig. S1). As we can see in Table 2, the bedrock and bare sediment classes are well classified in 2019 and 2021. There is more confusion between mixed vegetated areas and dense mature areas, with 2018 being the year with the least confusion. In all cases to test points, accuracy and kappa values show good results, with values higher than 92 % and 0.90 respectively.

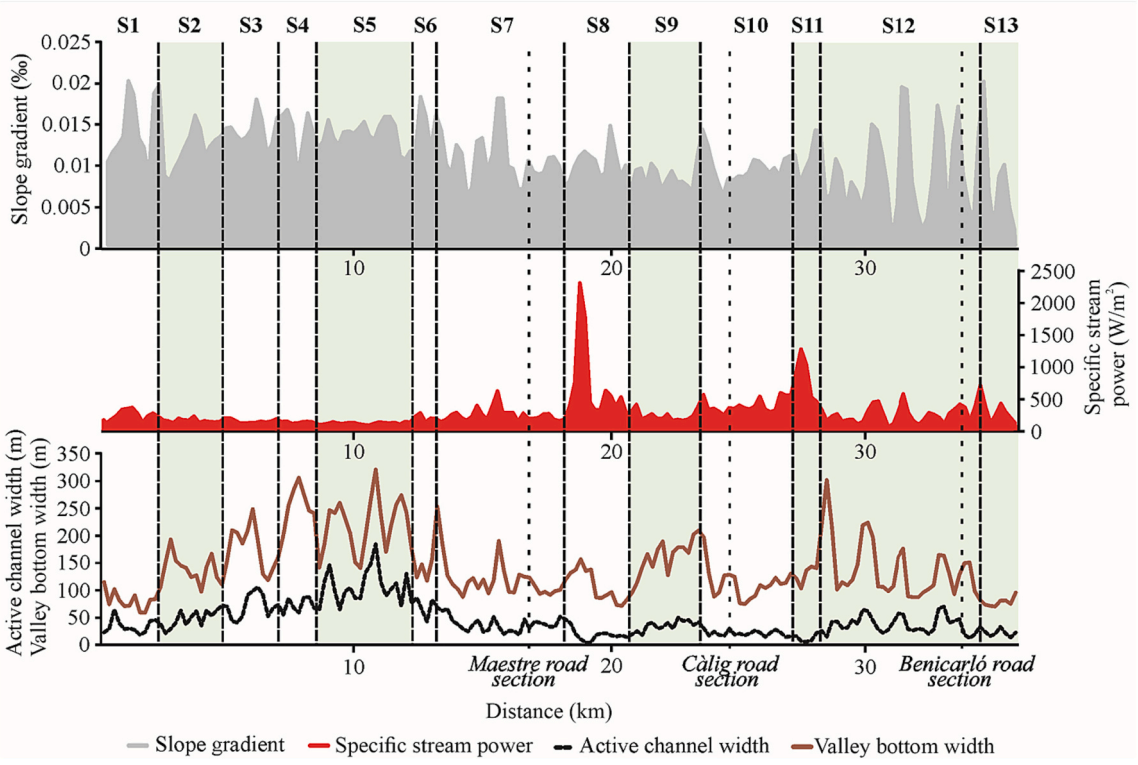

Fig. 3. Variables used for automatic segmentation showing their variation along the ephemeral stream and the segments obtained, representing the breaks with vertical dashed lines. Dashed vertical lines in S7, S10 and S12 refer to road sections where flow is measured by pressure transducers.

Table 2
Confusion matrix of supervised classification and accuracies. B: bedrock; BS: bare sediment; M: mixed vegetated areas; D: dense mature areas.

	2018				2019				2020				2021			
	B	BD	M	D	B	BD	M	D	B	BD	M	D	B	BD	M	D
B	21	0	0	0	21	0	0	0	20	1	0	0	21	0	0	0
BS	2	20	0	0	0	22	0	0	0	24	0	0	0	24	0	0
M	0	0	25	1	0	0	26	0	0	0	25	1	0	0	22	4
D	0	0	1	25	0	0	3	23	0	0	2	24	0	0	3	23
Accuracy	0.96				0.97				0.96				0.93			
Kappa	0.94				0.96				0.94				0.9			

In terms of automatic segmentation, the multivariate method yielded 13 statistically significant distinct segments (Fig. 3). These segments contain several of our reach length units (i.e., 200 m long subdivisions), the longest corresponding to segments S7 and S12 (Table S1), while the shortest with only a few length units are S4, S6, S11 and S13. Regarding the geomorphic characteristics of the segments, S3, S4, S5 and S6 have the widest active channel and valley bottom, while the narrowest active channel corresponds to S8, S10, S11 and S13. From S1 to S6, the specific stream power (SSP) values are very low due to the wider active channel and the highest SSP corresponds to S8 and S11 due to the narrower channel. In terms to the slope gradients, segments S3 to S6 have the highest values and then the values decrease downstream until S11 where they increase again. In S12 the slope gradient is locally high in relation to knickpoints and bedrock local steps. Finally, S13 has the lowest values of slope gradient of the river study.

4.2. Streamflow records

At the Cervera del Maestre (hereafter Maestre) and Benicarló sites (Fig. 3), flood water levels were recorded at 5-minute intervals and converted into discharges using a detailed 2D hydraulic model. The temporal frame was divided into three periods bracketed by the dates of the aerial photographs, typically taken in May or June. Three flow events occurred throughout the study period: 17 October 2018 (period 1) and 22 January and 1 April 2020 (period 2). There were no flow events between June 2020 and June 2021 (period 3).

At the Benicarló site, the 2018 flood hydrograph lasted for 33 h and consisted of two peaks of 170 m^3/s and 208 m^3/s that occurred 17 h apart (Fig. 4). In both peaks, the hydrograph shows a sharp rising limb and a progressive falling limb. At the Maestre site, the levelogger was destroyed by the flood, although the HWMs indicated a level of 1.61 m with an estimated discharge of 200 m^3/s.

Two major flow events were recorded in period 2. In January 2020, the flow showed a single hydrograph with a double peak, 3 h 30 min apart, observed at Maestre and Benicarló (Fig. 4). At the Maestre site, the flow lasted 17 h and reached a peak level of 1.1 m (80 m^3/s). In Benicarló the duration was 15 h with a peak discharge of 104 m^3/s (1.8 m stage). The April 2020 flow event at Benicarló showed a single peak hydrograph with a duration of 21 h and a peak of 223 m^3/s (stage 2.7 m). The hydrograph shows a sharp rising limb reaching its peak at 5 h and a falling limb at 16 h. At the Maestre site, the flow lasted 26 h with a maximum peak at a stage of 0.62 m, although in the falling part of the hydrograph a second peak reached 0.57 m (~200 m^3/s). Period 3 was not affected by any flow event and the channel changes are mainly related to vegetation growth.

4.3. Morphological changes along the study period: channel recovery variation along the river

Transition analysis (Fig. 5a) allows us to explore the river trajectories found along the study period based on channel recovery and vegetation encroachment rates. In general, the proportion of channel recovering dynamic landform features (e.g., open gravel bars) varies significantly along the study river (Fig. 6) ranging from 0.3 % in the case of segment S6 for the period 2020–2021 to 47.8 % in S11 for the period 2018–2019. In terms of vegetation encroachment, which favours the stabilisation of landforms, the proportion is lower, ranging from 0.6 % in the case of segment S11 for the period 2018–2019 to 17.3 % in the same segment

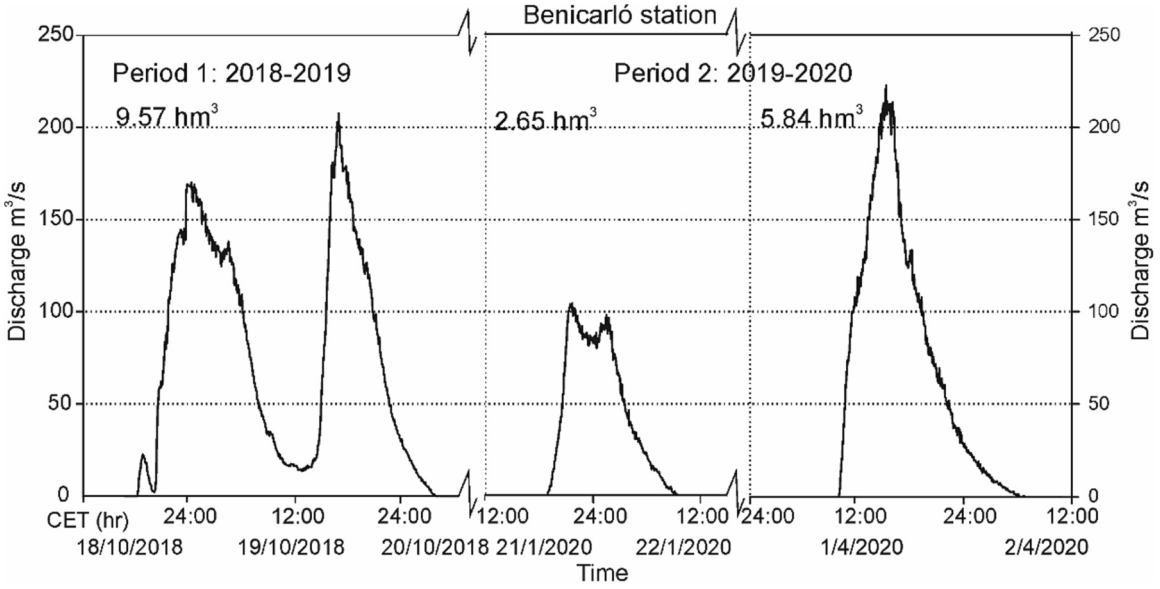

Fig. 4. Hydrographs of the flow events obtained by the stage-discharge relationship from 2D hydraulic modelling at the levelogger site in Benicarló. Note that flood 1 (left) corresponds to period 1, while floods 2 and 3 (centre and right) occurred during period 2.

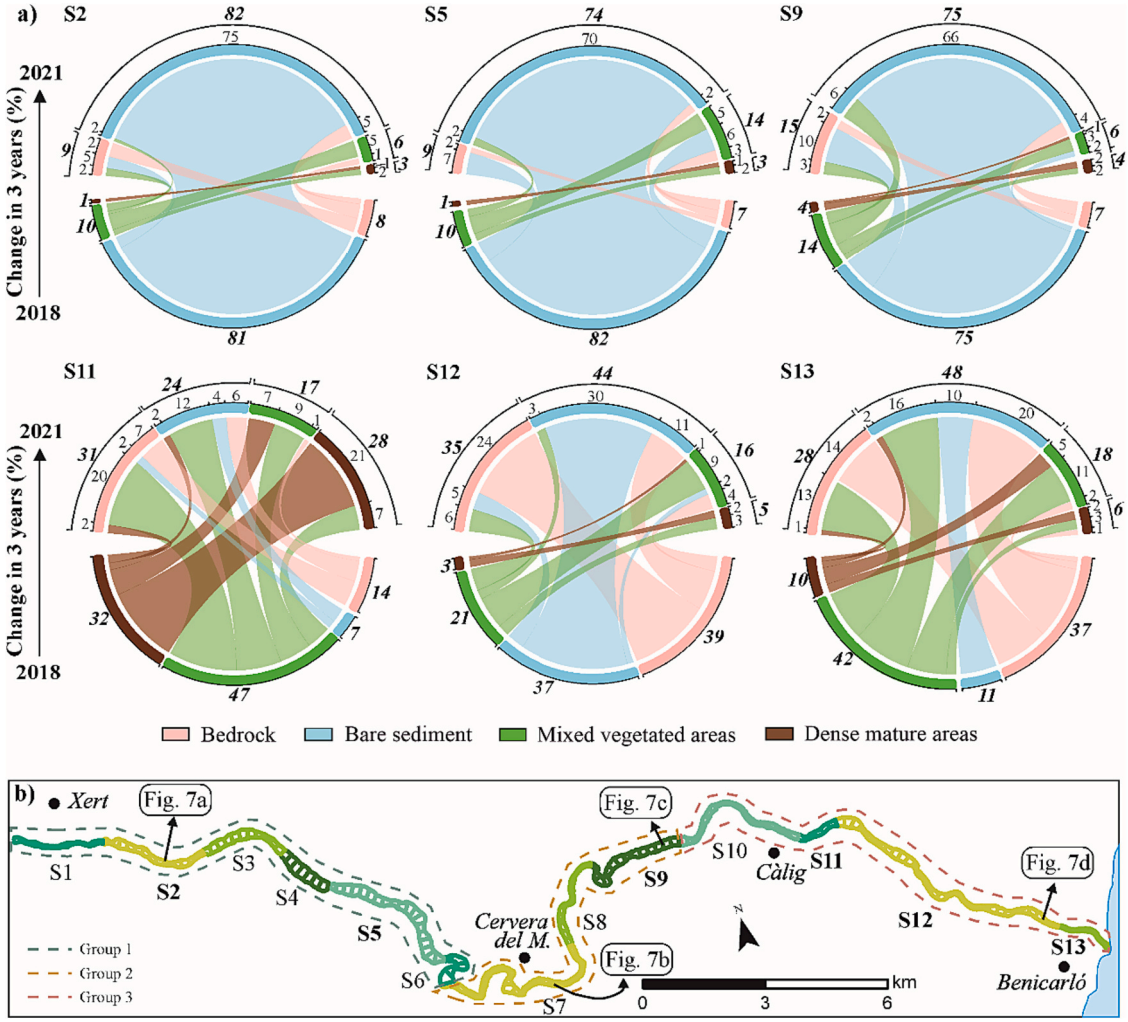

Fig. 5. a) Transition analysis in different segments along the river. Bold and italic numbers indicate the percentage of each category. b) Location of the 13 segments and boundaries of the segment groups (G1, G2 and G3) along the Rambla de Cervera.

(S11) for the period 2020–2021 (Fig. 6a).

Based on these spatio-temporal trajectories, three main groups of segments can be differentiated (Fig. 5b). This first group (G1) is composed of segments S1 to S6 and is characterised by the high proportion of surface remaining as bare sediment throughout the study period ranging from 82 % in 2018 to 74 % in 2021 in segment S5 (Fig. 5a), and presents the widest active channel (66.5 m on average with a maximum value of 105.9 m) (Figs. 6, 7a). This group shows a low channel recovery (~5 %) in the period 2018–2021 (Fig. 6b). As for vegetation encroachment, like channel recovery, it has very low values, although the percentage of S6 in the 2020–21 period is noteworthy with 12.2 % (Fig. 6a).

The second group (G2) comprises segments S7, S8 and S9 (Fig. 5b) and is also characterised by a relatively high proportion of surface remaining as channel and vegetated bars over the study period (around 66 % on average) (Fig. 5a), although the active channel is narrower (~30 m on average) (Figs. 6, 7b–c). This group G2 has a higher proportion of channel recovery than the previous ones (6.0 % on average between consecutive years) although a decreasing trend is observed in S7 from 8.2 % in 2018–2019 to 2.6 % in 2020–2021 (Figs. 6a, 8a). Meanwhile, the proportion of vegetation encroachment averages 4.9 % over the whole period (Fig. 6b), with an increasing trend (from 3.1 % in 2018–2019 to 7.9 % in 2020–2021) (Fig. 6a).

Finally, the third group, G3 extends from segment S10 to S13 (Fig. 5b), where a similar behaviour in terms of channel trajectories is observed compared to the second group although more pronounced for both variables (Figs. 6, 8). Channel recovery shows a decreasing trend along the period from 28.2 % in 2018–2019 to 2.9 % in 2020–2021 (Fig. 8a), while vegetation encroachment presents an increasing trend from 1.0 % to 11.8 % (Fig. 8b). The maximum channel recovery was recorded in S11 with 47.8 % in 2018–2019 (Fig. 6a), indicating that almost half of the channel surface was recovered in one year. This G3 group represents the narrowest active channel with an average of ~22 m (Figs. 6, 7d).

In summary, the analysis of the net trajectories for the entire period (i.e., 2018–2021) (Fig. 6b) shows that in G1 (S1 to S6) the proportions of channel recovery and vegetation encroachment are <7 %, with the exception of S6, which has a vegetation encroachment of 15.7 % for the entire period (Fig. 6b). In G2 (S7 to S9) the net channel recovery over the whole period is more remarkable, with values of 12.9 % in S8 and 9.7 % in S9, with vegetation encroachment <10 %. The G3 shows the highest net channel recovery, with values of 33.9 % and 31.3 % in S11 and S13 respectively, while vegetation encroachment is <7 % (Fig. 6b).

4.4. Relationships between hydraulics and geomorphology

Short- and medium term geomorphic changes are related to the flow energy input during annual floods and thus to the sequence of peak flows and flow duration. In general, the cumulative flow energy calculation for a flood hydrograph is a proxy for the geomorphic work of each flood

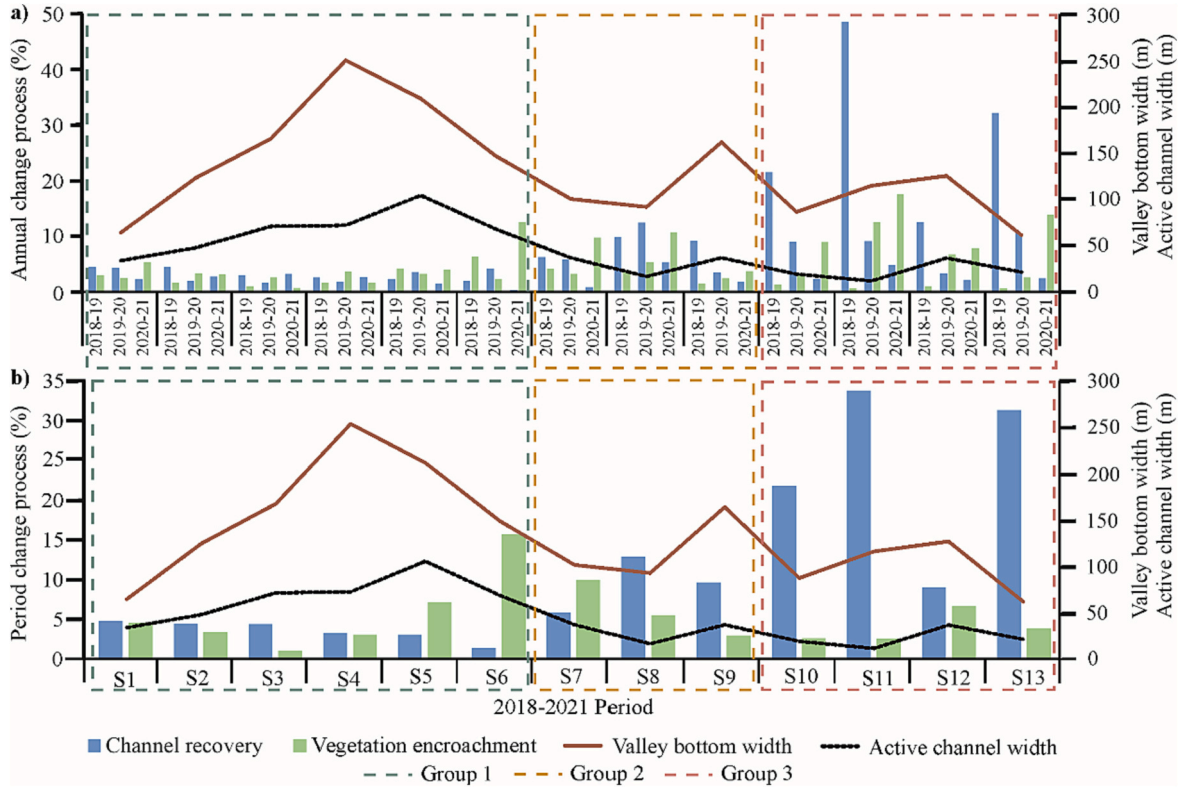

Fig. 6. a) Annual channel recovery and vegetation encroachment percentage for the periods 2018–2019, 2019–2020 and, 2020–2021 periods. b) Channel recovery and vegetation encroachment percentage for the entire study period (2018–2021).

event (Lekach and Enzel, 2021). In the first period (2018–19), the maximum peak discharge was 210 m^3/s with a total power of 10,400 watts. In the second period (2019–20), the two flood events (104 and 223 m^3/s) result in a cumulative power of 2880 and 6360 watts, respectively. At the local scale, the reconstruction of these flow conditions, combined with mapped and measured changes in landform units, provides a quantitative relationship between hydraulic conditions and resulting erosional and depositional features (e.g., vegetation to channel, vegetation to bedrock, Fig. 9).

In the G1 segments, the flow width during the recorded floods occupied the most active parts of the river corridor, i.e., the bare sediment, with a shear stress of 50–100 N/m^2 (Figs. S3–S5) and a maximum velocity of 3–3.5 m/s (Figs. S8–S10). In the mixed and dense mature vegetated bars, the flow velocity was <1 m/s and the shear stress <20 N/m^2, even during the largest floods (210–223 m^3/s). These hydraulic conditions explain the limited alluvial expansion observed in the first and second periods, and even a contraction due to vegetation growth in the third period associated with the lack of flow. The changes from shrub vegetation to bare alluvial cover occurred on partially vegetated bars attached to the channel margin and on central diagonal bars under relatively shallow flows (<0.3 m), with mean velocity of 1.5–2.3 m/s and shear stress <60 N/m^2 (Fig. 9). Interestingly, the geomorphic work required to change from vegetated areas to bedrock exposure was less than that required to change to bare alluvial cover, with velocities <1.6 m/s and shear stress <35 N/m^2. It should be noted that the change from vegetation to alluvial cover occurred mainly within the floodplain, whereas the change to bedrock occurred at the edge of the floodplain under shallow soil or alluvium.

In the G2 segments, the main flow extended from the gravel channel to the vegetated bars even during the lowest flow event (~100 m^3/s). For example, in the lateral secondary channel our model shows shear stresses of 100–200 N/m^2 (Figs. S11–S13) and flow velocities of 2.5–3 m/s (Figs. S17–S19). During the largest flow events (2018 and April 2020), the channel banks and vegetated bar islands recorded the highest modelled shear stress (300–400 N/m^2), explaining the trend of alluvial surface expansion during flood events. Conversely, during the third period (2020−2021), when there was no flow, vegetation growth resulted in significant encroachment, particularly in segments S7 and S9. Changes from vegetated surfaces to bedrock were more frequent than to fresh bare alluvium. In both cases the energy conditions with shift to bedrock and bare alluvial surfaces were not so different with an average depth of 0.5–1 m (Figs. S14–S16), velocity of 2–3.5 m and shear stress between 50 and 80 N/m^2 (Fig. 9). Note that these hydraulic values are higher than those required for similar changes in the G1 segments.

In the G3 segments, the main channel areas convey high energy flow conditions with shear stress >100 N/m^2 (Figs. S20–S22) and flow velocity > 3.5 m/s (Figs. S26–S28), reaching >300 N/m^2 and velocity of 6 m/s in the pool areas. During high flow conditions, water overflows the valley sides with secondary channels and high, rough bedrock surfaces that dissipate flow energy and form transverse ridges, suggesting the formation of standing waves. In S12, the 2018 flow of ~210 m^3/s was able to remove shrub and tree vegetation and increase the bedrock and alluvial surface area. The change from vegetation to bedrock occurred even in lateral valley areas under relatively low mean depth (0.30 m), velocity (1.2 m/s) and shear stress (30 N/m^2) values, whereas the change from vegetation to alluvial channel required slightly higher energy conditions (Fig. 9). Most of the changes from vegetation to alluvium are at the bottom of the main channels, probably related to deposition in the recession limb of the hydrograph. Changes from vegetation to bedrock are typically on the banks of the main channel and at the channel bottom, where seasonal shrub vegetation has moved into the bedrock erosion classes. During the 2020 floods, the total area converted from vegetation to bedrock or alluvium was only 40 % of the previous period and was mainly located on the bottom of secondary channels and on the sides of the main channel. These changes are consistent with the slight decrease in the proportion of vegetation encroachment and

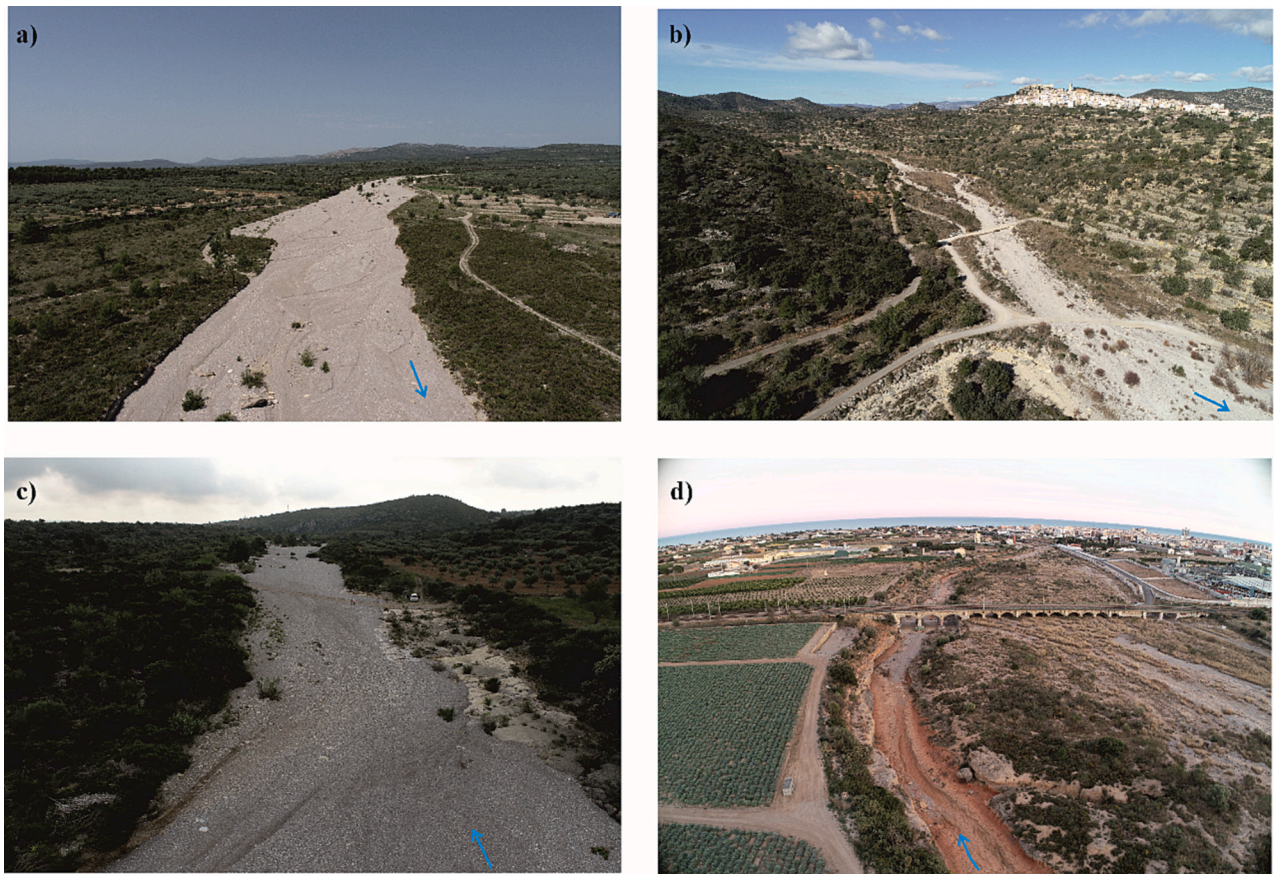

Fig. 7. UAV aerial view of representative segments of the three river groups (G), note that the blue arrow indicates the direction of the flow. a) Upstream view of the S2 segment, representing G1 wide alluvial setting in the graben structural constraint. b) Upstream view of the narrow active channel with multiphase gravel surfaces incised on structurally controlled limestone bedrock (horst) representing G2. c) Downstream view of the S9 segment, with shallow gravel deposits covering bedrock exposed surfaces at the transition between G2 and G3. d) Downstream view of the S12 segment showing a wide river corridor with a deep innerchannel incised on the Pleistocene cemented gravel bedrock. The Mediterranean Sea is in the background. Note the scattered gravel bars on a general bedrock incised channel on the left river corridor. Overbank flow on the right valley margin occurs during medium to large flows and produces crevasse splay gravel accumulation.

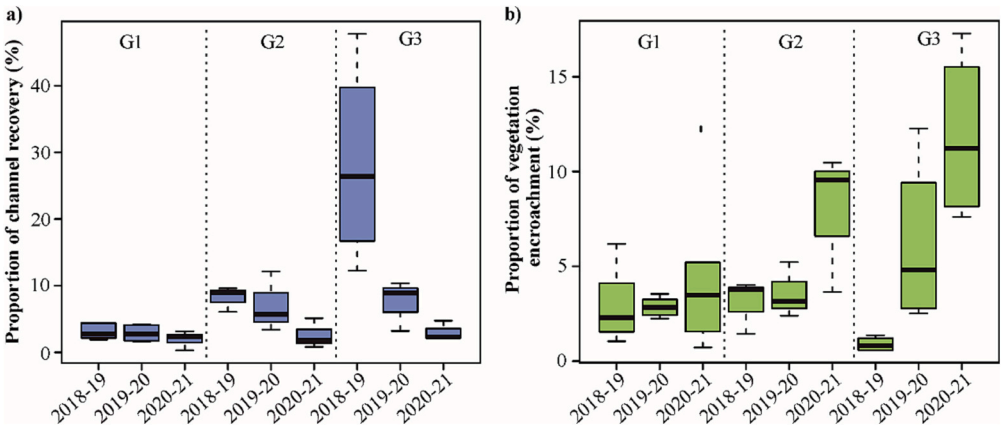

Fig. 8. Boxplots showing the proportion of change over the study period for the three groups described (G1: Group 1, G2: Group 2, G3: Group 3). a) Proportion of channel recovery and b) Proportion of the vegetation encroachment.

channel recovery observed in the second period (2019–20) within the G3 segments (Fig. 8). The absence of floods in the third period (2020−21) explains both the increase in vegetation encroachment and the decrease in channel recovery, indicating the importance of floods in the overall recovery of hydromorphological conditions in the G3 segments.

5. Discussion

Our methodological approach to quantifying channel recovery in ephemeral rivers affected by gravel extraction has allowed us to analyse the changes that have occurred over a short period of time and to understand which flows are likely to be responsible for these changes. In this section, we discuss the natural response and geomorphic sensitivity

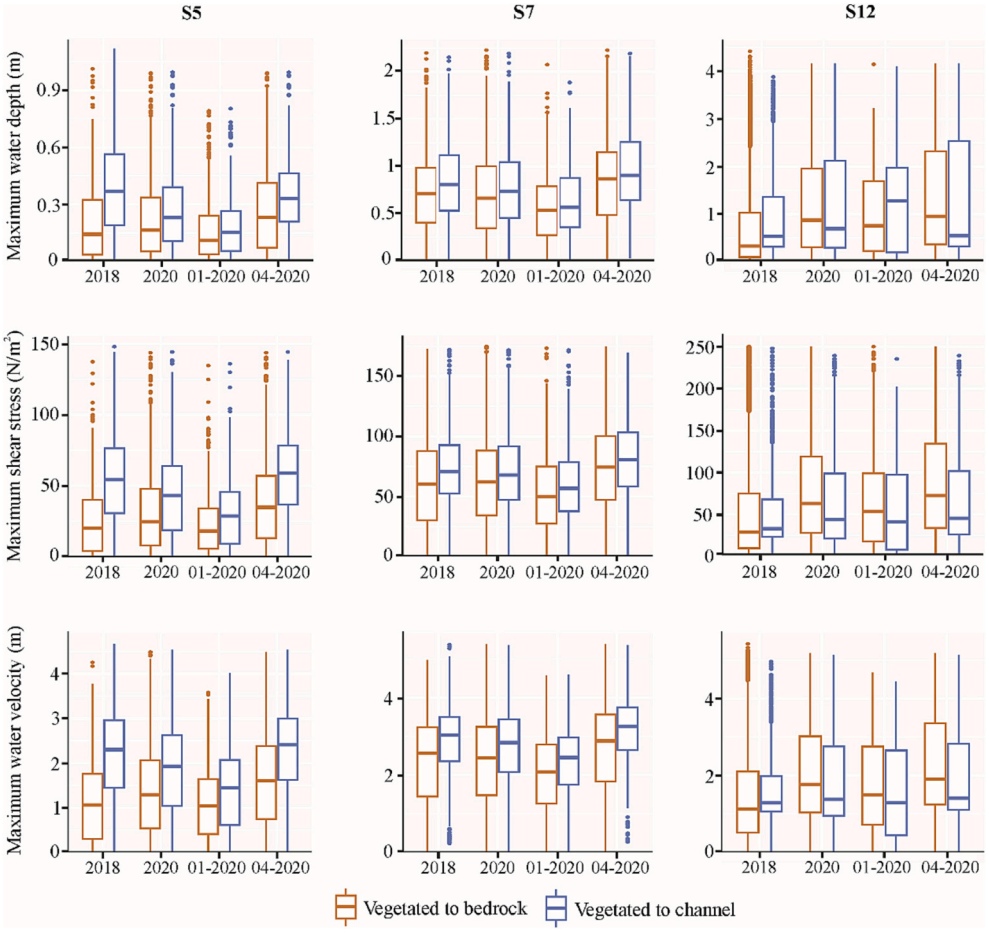

Fig. 9. Boxplots showing the mean and standard deviation of hydraulic parameters (depth, velocity and shear stress) at peak discharge associated with changes from vegetated areas to bedrock and to channel in representative segments of G1, G2 and G3.

to change by considering channel recovery, degradation and landform stabilisation by vegetation (see Section 5.1). The changes in channel recovery and vegetation encroachment over the entire period (2018–2021) are then used to conceptualise the evolution of different trajectories representing recovery scenarios (see Section 5.2).

5.1. *Short-term geomorphic response and sensitivity to river recovery*

Our results show that the study stream is sensitive to changes caused by floods during the short-term period analysed (2018 to 2021), which occur mainly in the degraded segments of the study stream. This is because the sediment size is smaller than in the other segments and the sensitivity depends on the sediment size of the channel (Hooke, 2016b). That is why the most degraded segments present net channel recoveries above 30 %, i.e., new areas of gravel bars previously stabilised by vegetation, and with low stabilisation by vegetation encroachment (around 7 %). According to Fryirs and Brierley (2000), river recovery refers to the adjustment processes to improve geomorphic condition following disturbance. Evidence of recovery is based on the landform sequence (lateral and longitudinal) expected for the natural conditions under current physical constraints. The definition of what is natural in rivers after a severe human modification has been a point of debate in river restoration analysis (Wohl and Merritts, 2007; Gregory, 2019). On the one hand, it is important to establish the river condition under the concept of the historical range of variability (Fuller et al., 2021) and the river recovery potential under current dynamic constraints (Fryirs and Brierley, 2000; Brierley et al., 2002). In this respect, the post-disturbance physical boundaries have conditioned the short-term dynamic processes (i.e., flow, sediment flux and vegetation cover) constraining the possible range of channel change behaviour (Cluer and Thorne, 2013). The analysis of short-term geomorphic processes is critical to ascertain the extent, time scales, and trajectories of adjustment when assessing the river recovery potential (see Fryirs and Brierley, 2000) and their sensitivity to change. Our approach takes advantage of the annually repeated high-resolution aerial imagery available from open-source repositories to analyse the geomorphic response of degraded rivers to specific flows at the catchment scale. This approach is based on a two-step procedure (Rabanaque et al., 2022): (1) river network segmentation, which focuses on the distribution of reaches with similar geomorphological, geometric and hydraulic attributes, and (2) diachronic landform analysis, which combines remote sensing and machine learning techniques to obtain a semi-automatic fluvial landform mapping with an objective criterion. This wide-basin analysis provides an efficient way to obtain a homogeneous and coherent mapping of landform and vegetation to monitor geomorphic changes and trajectories in response to hydrological events.

The multivariate segmentation was assigned to three channel types on the basis of geomorphical and hydraulic parameters, according to the classification of Mediterranean ephemeral streams (Rabanaque et al., 2022). These channel types show a spatial distribution that depends on geological and structural factors (graben vs horst areas) but with a secondary control related to geomorphological changes induced by anthropogenic activities (gravel mining in this case). This mainly involves a deep channel incision and sediment depletion towards the lowest reaches (Fig. 10). The Group 1, segments (S1 to S6), is located in a graben (depression) sector with a low degree of channel confinement,

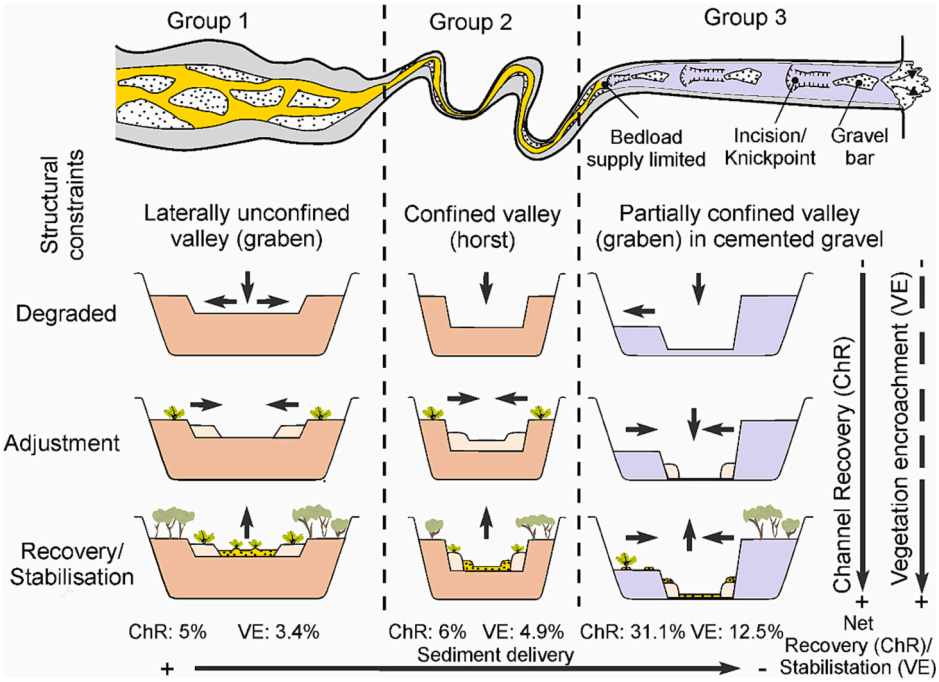

Fig. 10. Spatial and temporal structural and dynamic constraints and recovery trajectories of channels following disturbance.

although disturbance conditions have caused incision of the active alluvial channel on former the floodplain, limiting its lateral expansion and shifting (Fig. 7a). According to the regional channel classification of Rabanaque et al. (2022), these segments are channel types 3 and 4, consisting of a wide active channel with longitudinal, lateral and transverse gravel bars, and mixed vegetated areas. In these G1 segments, any change in sediment and water fluxes, either natural or human induced, would imply an adjustment of the channel to the new equilibrium (Downs and Gregory, 2004). Clearly, this first group is in the best geomorphic condition compared to the other groups (G2 and G3) with the exception of S1, which is deeply incised (Segura-Beltrán et al., 2020). The diachronic analysis shows that geomorphic changes over two flow periods are minor or absent (Rabanaque et al., 2021). The wide active channel produces shallow flow with low SSP, implying a reduction in overbank flow and disconnection of floodplains, except during extreme flows. Therefore, G1 segments are geomorphologically more effective but less sensitive, i.e., small and moderate flows are able to transport sediment and activate gravel bar migration, which in terms of diachronic analysis results in minor net channel landform changes over the study period (Figs. 6, 8). Group G2, formed by segments S7 to S9, is located in a horst (range) sector (Fig. 10) and includes channel types 2 and 3 following Rabanaque et al. (2022) classification. These types show a high channel confinement characterised by a narrow active channel with medium values of SSP. The channel platform includes an alternation of scour pools and lobe bars, denoting depletion on gravel bedload. Channel narrowing increases the occurrence of overbank flow, even at low/medium flows, enhancing the reconnection through vegetation removal (Croke et al., 2017). As a result, G2 is geomorphologically sensitive with an enhanced response to low/medium flows (Figs. 6, 8), albeit within a general sediment depletion condition characterised by coarse gravel bars and islands colonised by vegetation (Fig. 7b–c).

The most downstream group (G3) comprises segments S10 to S13 located in a graben sector (Fig. 10), which means that the segment types should be similar to G1 (i.e., types 3 and 4; Rabanaque et al., 2022). However, the pre-1950s alluvial channel has been severely affected by gravel extraction since the 1980s (Segura-Beltrán and Sanchis-Ibor, 2013), resulting in a single channel deeply incised on bedrock-cemented gravels (Fig. 7d). The present channel platform consists of an alternation of scour pools, or incised inner-channel often featuring knickpoints, and lobe bars that decrease in length downstream as sediment availability decreases. In the long-term, G3 has been very sensitive to human-induced changes, resulting in a persistent, severe morphological change that is conducive to a high degradation and the creation of a new river condition (i.e., non-turning point; Fryirs and Brierley, 2000). In the recent short-term, morphodynamic sensitivity has been suppressed and translated into process sensitivity (Downs et al., 2013) characterised by (1) increased sediment transport capacity within an entrenched channel and (2) uncharacteristic floodplain scour features with crevasse splays, gravel sheet deposition and rugged bedrock exposure. Channel recovery observed over the study period includes vegetation removal and deposition of lobes and gravel patches associated with high flow velocities even during low moderated floods. As the potential for morphodynamic sensitivity is high, the main limiting factors for recovery in G3 segments are (1) the lack of sediment flux, which would require high rates of longitudinal sediment delivery for effective recovery, and (2) the scarcity of sediment storage on river banks and floodplains. Therefore, recovery of G3 segments would imply to identify the multiple spatio-temporal drivers and channel possible trajectories for naturalisation according to contemporary fluvial processes (Kondolf et al., 2006; Fryirs and Brierley, 2016).

5.2. *Lessons learned towards Mediterranean ephemeral streams recovery*

One of the key questions in rivers affected by human alterations is whether recovery is possible in severely degraded rivers. The short-term changes found in this study suggest that fluvial process conditions are excellent, but that a stimulus is needed to increase sediment delivery from upstream reaches to create river landforms. As the river network is composed of different channel types with different sensitivities and degrees of degradation, the character and mechanisms of recovery are interrelated, implying the need for a catchment scale approach. On the one hand, G1 segments are geomorphologically insensitive to moderate flows, at least in the short-term, implying that they are morphodynamically resilient and that management efforts should focus on their conservation (e.g., Downs et al., 2013). This idea is consistent with the findings of Scamardo et al. (2023), whose results showed that the

river corridor is an important predictor of geomorphic heterogeneity, defined as the temporal and spatial variability of geomorphic units, i.e., the wider the river corridor, the higher the probability of high dynamics. In contrast, G3 maintains reach-scale processes, but recovery would require restoration of physical processes within the catchment (i.e., G1 and G2), namely sediment production and connectivity, from which it would tend to return the channel to more 'natural' conditions (e.g., Kondolf et al., 2006). Such recovery may take decades even in this high-energy Mediterranean ephemeral stream, whereas 'naturalisation' may be accelerated by removing existing human and geomorphological barriers (e.g., road crossings, morphological-vegetation encroachments). In this task, our methodological approach of short-term morphodynamic analysis provides an effective tool to monitor reach-differentiated process responses and their sensitivity. For example, current asynchrony between sediment load and flow peaks due to hungry water is evidenced by discontinuous alluvial landforms and gravel patches along the G3 channel. Therefore, recovery from the dominant erosion processes in G3 is likely to occur when gravel bars cover much of the active channel. An important lesson from the analysis of short-term changes is that improved morphodynamic conditions and processes (e.g., sediment delivery) in upstream reaches (e.g., G2) would be required before further direct management interventions could be undertaken in the most degraded reaches. It is therefore important that the setting of the degraded reach within the catchment is properly assessed (England and Gurnell, 2016).

The lack of sediment supply is a direct consequence of decades of mining in the river. However, this is complemented by the effects of changes in land use and land cover (LULC) (Gregory et al., 2006). Since the mid-20th century, forest cover in the basin has increased to 33 %, reaching 53 % in the headwaters (Segura-Beltrán and Sanchis-Ibor, 2013). The abandonment of agricultural land has also led to natural regeneration of vegetation, mainly shrubs, which serve as a transition stage to full forest cover (Rodriguez-Lloveras et al., 2016). Such LULC changes typically lead to a decrease in water runoff and sediment production, and therefore to a decrease in bedload and river morphodynamics (e.g., García-Ruiz and Lana-Renault, 2011; Sanchis-Ibor et al., 2017). A conceptual change for river restoration in reaches with sufficient capacity to transport bedload material, but with a lack of sediment supply, will involve actions at the catchment scale. For example, the removal of existing dams and barriers would increase sediment supply to the main river and create conditions to improve sediment supply to the most downstream segments. The removal, realignment or modification of sediment retention structures have been proposed in the European Guidelines for Integrated Sediment Management (Ausili et al., 2022) as measures to address deficiencies in sediment supply, continuity and local hydromorphological changes. These nature-based solutions will enhance and improve natural sediment transport processes, resulting in the strategic restoration of hydromorphological connectivity.

6. Conclusions

Decades of intensive gravel extraction in Mediterranean ephemeral channels have resulted in highly altered hydromorphological conditions, posing a major challenge to fluvial recovery. Such drastic geomorphic changes strengthen the case for addressing geomorphic restoration at the scale of contemporary fluvial processes rather than historical pre-disturbance conditions (e.g., Fryirs and Brierley, 2000; Downs et al., 2013). Monitoring contemporary evolutionary channel trajectories requires an understanding of short-term morphological changes and their reach-specific physical constraints and process-form responses. In this study, we apply a combination of (1) automated stream segmentation using LiDAR-derived geometric and hydraulic variables, (2) landform classification from remote sensing and machine learning algorithms to quantify reach-scale morpho-dynamic changes, and (3) 2D hydraulic modelling of the three flow hydrographs recorded during 2018–2021.

Thirteen segments were identified along the 44 km long study channel of the Rambla de Cervera (340 km^2), divided into three groups (G1 to G3) according to their structural valley setting and sensitivity to channel morphodynamic response. The upstream G1 segments, with a wide unconfined alluvial bed, showed little change between landform classes, implying low values of channel recovery and vegetation encroachment. This segment behaviour reflects minor geomorphic adjustments (i.e., water and sediment flows and vegetation interactions) with limited flow energy capacity expended on bedload transport and active bar migration. The confined setting of G2 segments showed higher net alluvial changes (channel recovery) and vegetation encroachment proportions than G1. These changes are associated with a higher incidence of overbank flow, even during moderate annual flows, which increases geomorphic sensitivity, albeit with a general sediment depletion towards downstream segments. The most downstream group, G3, showed the greatest changes in landform classes, both in terms of alluvial/rock exposure and vegetation encroachment. However, this G3 consists of a discontinuous, deeply incised channel on bedrock with multiple knickpoints, representing an insensitive (resilient) landscape heavily impacted by gravel extraction since the 1970s. Here the hydraulic model shows very high energy conditions and an erosional process domain with hungry water indicated by discontinuous landforms and gravel patches. In this highly modified landscape, induced by human disturbance, it is otherwise incapable of storing sediment or producing persistent alluvial landforms to improve the geomorphological condition. In terms of management, G1 and G2 segments are morpho-dynamically resilient and management actions are required to maintain them, whereas G3 shows irreversible changes and restoration to more 'natural' conditions is only possible by increasing sediment supply from upstream reaches.

The diversity of channel response and sensitivity between segment groups highlights the importance of addressing river recovery and restoration at large spatial scales (e.g., (Downs et al., 2013; Fryirs, 2017). Finally, the increasing availability of repeated remote sensing imagery in the future would help to better estimate rates of river recovery after floods of different magnitudes. Monitoring changes in ephemeral rivers provides very important information to know the state of these rivers or to implement measures to mitigate the effects of anthropogenic activities.

Funding

This work is supported by the Ministry of Science and Innovation (MCIN/AEI/10.13039/501100011033), co-financed by the FEDER funds through the EPHIDREAMS project (PID2020-116537RBI00), and by the Directorate General of Water (DGA) of the MITERD (Grant 20223TE002).

CRediT authorship contribution statement

Maria Pilar Rabanaque: Writing – review & editing, Writing – original draft, Validation, Software, Methodology, Investigation, Formal analysis, Conceptualization. **Vanesa Martínez-Fernández:** Writing – review & editing, Writing – original draft, Validation, Software, Methodology, Investigation, Formal analysis, Conceptualization. **Mikel Calle:** Writing – review & editing, Writing – original draft, Validation, Software, Methodology, Investigation, Formal analysis, Conceptualization. **Olegario Castillo:** Writing – review & editing, Writing – original draft, Software, Methodology. **Gerardo Benito:** Writing – review & editing, Writing – original draft, Supervision, Project administration, Investigation, Funding acquisition, Conceptualization.

Declaration of competing interest

The authors declare no competing interests.

Data availability

Data will be made available on request.

Acknowledgements

The research conducted in this study was funded by the Ministry of Science and Innovation through the EPHIDREAMS project (PID2020-116537RBI00), funded by the Ministry of Science and Innovation MCIN/AEI/10.13039/501100011033, co-financed with FEDER funds, and by the General Water Directorate (DGA) of the MITERD (Grant MNCN-CSIC 20223TE002). M.P. Rabanaque was funded by contracts from the Spanish Ministry of Science and Innovation, namely from the PhD FPI programme (PRE2018-086771). M. Calle was partially financed by the EPHIDREAMS project, Turku Collegium of Science, Medicine and Technology (TCSMT) and Hydro-RDI-Network, Academy of Finland funding ID: 337279. This work is part of the CSIC-PTI TELEDETECT activity. This article is a contribution of the Hydrology and Climate Change Laboratory (www.floodsresearch.com; Twitter: floods_research; Instragram: @floods_research). Finally, the authors would like to thank the editor and the two reviewers for their helpful suggestions.

Appendix A. Supplementary data

Supplementary data to this article can be found online at https://doi.org/10.1016/j.geomorph.2024.109069.

References

Alber, A., Piégay, H., 2011. Spatial disaggregation and aggregation procedures for characterizing fluvial features at the network-scale: Application to the Rhône basin (France). Geomorphology 125, 343–360. https://doi.org/10.1016/j.geomorph.2010.09.009.

Anadón, P., Moissenet, E., 1996. Neogene basins in the Eastern Iberian Range. In: Dabrio, C.J., Friend, P.F. (Eds.), Tertiary Basins of Spain: The Stratigraphic Record of Crustal Kinematics, World and Regional Geology. Cambridge University Press, Cambridge, pp. 68–76. https://doi.org/10.1017/CBO9780511524851.013.

Ausili, A., Borowiec, P., Boughaba, J., Branche, E., Brils, J., Brinke, M., Brooke, J., Bussettini, M., Carere, M., Carls, I., Casado Martinez, M.C., Clayton, H., Cleveringa, J., Comiti, F., David, S., Dokkum, R., Dudas, K., Ferrer, C., Goltara, A., Winterscheid, A., 2022. Integrated Sediment Management (Guidelines and good practices in the context of the Water Framework Directive).

Batalla, R.J., 2003. Sediment deficit in rivers caused by dams and instream gravel mining. Are view with examples from NE Spain. Cuaternario y geomorfología: Revista de la Sociedad Española de Geomorfología y Asociación Española para el Estudio del Cuaternario 17, 79–91.

Batalla, R.J., Vericat, D., Martínez, T.I., 2006. River-channel changes downstream from dams in the lower Ebro River. Zeitschrift fur Geomorphologie, Supplementband 1–15.

Beechie, T.J., Sear, D.A., Olden, J.D., Pess, G.R., Buffington, J.M., Moir, H., Roni, P., Pollock, M.M., 2010. Process-based Principles for Restoring River Ecosystems. BioScience 60, 209–222. https://doi.org/10.1525/bio.2010.60.3.7.

Bizzi, S., Lerner, D.N., 2012. Characterizing physical habitats in rivers using map-derived drivers of fluvial geomorphic processes. Geomorphology 169–170, 64–73. https://doi.org/10.1016/j.geomorph.2012.04.009.

Bladé, E., Cea, L., Corestein, G., Escolano, E., Puertas, J., Vázquez-Cendón, E., Dolz, J., Coll, A., 2014. Iber: herramienta de simulación numérica del flujo en ríos. Revista Internacional de Métodos Numéricos para Cálculo y Diseño en Ingeniería 30, 1–10. https://doi.org/10.1016/j.rimni.2012.07.004.

Breiman, L., 2001. Random Forests. Mach. Learn. 45, 5–32. https://doi.org/10.1023/A:1010933404324.

Brierley, G., Fryirs, K., Outhet, D., Massey, C., 2002. Application of the River Styles framework as a basis for river management in New South Wales, Australia. Appl. Geogr. 22, 91–122. https://doi.org/10.1016/S0143-6228(01)00016-9.

Brierley, G.J., Fryirs, K.A., 2016. The use of Evolutionary Trajectories to Guide 'moving Targets' in the Management of River Futures. River Res. Appl. 32, 823–835. https://doi.org/10.1002/rra.2930.

Brunsden, D., Thornes, J.B., 1979. Landscape Sensitivity and Change. Trans. Inst. Br. Geogr. 4, 463–484. https://doi.org/10.2307/622210.

Calle, M., Alho, P., Benito, G., 2017. Channel dynamics and geomorphic resilience in an ephemeral Mediterranean river affected by gravel mining. Geomorphology 285, 333–346. https://doi.org/10.1016/j.geomorph.2017.02.026.

Calle, M., Calle, J., Alho, P., Benito, G., 2020. Inferring sediment transfers and functional connectivity of rivers from repeat topographic surveys. Earth Surf. Process. Landf. 45, 681–693. https://doi.org/10.1002/esp.4765.

Carbonneau, P.E., Dugdale, S.J., Breckon, T.P., Dietrich, J.T., Fonstad, M.A., Miyamoto, H., Woodget, A.S., 2020. Adopting deep learning methods for airborne RGB fluvial scene classification. Remote Sens. Environ. 251, 112107 https://doi.org/10.1016/j.rse.2020.112107.

CEDEX, 2013. Mapa de caudales máximos del España Peninsular (CAUMAX).

Cluer, B., Thorne, C., 2013. A Stream Evolution Model Integrating Habitat and Ecosystem Benefits. River Res. Appl. 30, 135–154. https://doi.org/10.1002/rra.2631.

Cortes, C., Vapnik, V., 1995. Support-vector networks. Machine Learning 20, 273–297. https://doi.org/10.1007/BF00994018.

Croke, J., Thompson, C., Fryirs, K., 2017. Prioritising the placement of riparian vegetation to reduce flood risk and end-of-catchment sediment yields: Important considerations in hydrologically-variable regions. J. Environ. Manage. 190, 9–19. https://doi.org/10.1016/j.jenvman.2016.12.046.

Datry, T., Bonada, N., Boulton, A.J., 2017. What are intermittent rivers and ephemeral streams (IRES)? In: Datry, T., Bonada, N., Boulton, A.J. (Eds.), Intermittent Rivers and Ephemeral Streams. Ecology and Management. Elsevier, United Kingdom, pp. 01–16.

Downs, P.W., Gregory, K.J., 2004. River Channel Management: Towards Sustainable Catchment Hydrosystems. Routledge, London.

Downs, P.W., Dusterhoff, S.R., Sears, W.A., 2013. Reach-scale channel sensitivity to multiple human activities and natural events: lower Santa Clara River, California, USA. Geomorphology 189, 121–134. https://doi.org/10.1016/j.geomorph.2013.01.023.

Dufour, S., Piégay, H., 2009. From the myth of a lost paradise to targeted river restoration: forget natural references and focus on human benefits. River Res. Appl. 25, 568–581. https://doi.org/10.1002/rra.1239.

England, J., Gurnell, A.M., 2016. Incorporating catchment to reach scale processes into hydromorphological assessment in the UK. Water and Environment Journal 30, 22–30. https://doi.org/10.1111/wej.12172.

Escadafal, R., Huete, A., 1991. Etude des propriétés spectrales des sols arides appliquée à l'amélioration des indices de végétation obtenus par télédétection. Comptes rendus de l'Académie des Sciences. Série 2 Mécanique 312, 1385–1391.

European Commission (EC), 2000. Directive 2000/60/EC of the European Parliament and of the Council Establishing a Framework for Community Action in the Field of Water Policy. Office for Official Publications of the European Communities, Luxembourg.

Fryirs, K., Brierley, G., 2000. A Geomorphic Approach to the Identification of River Recovery potential. Phys. Geogr. 21, 244–277. https://doi.org/10.1080/02723646.2000.10642708.

Fryirs, K.A., 2017. River sensitivity: a lost foundation concept in fluvial geomorphology. Earth Surf. Process. Landf. 42, 55–70. https://doi.org/10.1002/esp.3940.

Fryirs, K.A., Brierley, G.J., 2016. Assessing the geomorphic recovery potential of rivers: forecasting future trajectories of adjustment for use in management. WIREs Water 3, 727–748. https://doi.org/10.1002/wat2.1158.

Fuller, I.C., Death, R.G., Garcia, J.H., Trenc, N., Pratt, R., Pitiot, C., Matoš, B., Ollero, A., Neverman, A., Death, A., 2021. An index to assess the extent and success of river and floodplain restoration: Recognising dynamic response trajectories and applying a process-based approach to managing river recovery. River Res. Appl. 37, 163–175. https://doi.org/10.1002/rra.3672.

Gallart, F., Cid, N., Latron, J., Llorens, P., Bonada, N., Jeuffroy, J., Jiménez-Argudo, S.-M., Vega, R.-M., Solà, C., Soria, M., Bardina, M., Hernández-Casahuga, A.-J., Fidalgo, A., Estrela, T., Munné, A., Prat, N., 2017. TREHS: an open-access software tool for investigating and evaluating temporary river regimes as a first step for their ecological status assessment. Sci. Total Environ. 607–608, 519–540. https://doi.org/10.1016/j.scitotenv.2017.06.209.

García-Ruiz, J.M., Lana-Renault, N., 2011. Hydrological and erosive consequences of farmland abandonment in Europe, with special reference to the Mediterranean region - a review. Agric. Ecosyst. Environ. 140, 317–338. https://doi.org/10.1016/j.agee.2011.01.003.

Gregory, K.J., 2019. Human influence on the morphological adjustment of river channels: the evolution of pertinent concepts in river science. River Res. Appl. 35, 1097–1106. https://doi.org/10.1002/rra.3455.

Gregory, K.J., Benito, G., Dikau, R., Golosov, V., Johnstone, E.C., Jones, A.J.J., Macklin, M.G., Parsons, A.J., Passmore, D.G., Poesen, J., Soja, R., Starkel, L., Thorndycraft, V.R., Walling, D.E., 2006. Past hydrological events and global change. Hydrol. Process. 20, 199–204. https://doi.org/10.1002/hyp.6105.

Gu, Z., 2022. circlize: Circular Visualization.

Hooke, J.M., 2016a. Geomorphological impacts of an extreme flood in SE Spain. Geomorphology 263, 19–38. https://doi.org/10.1016/j.geomorph.2016.03.021.

Hooke, J.M., 2016b. Morphological impacts of flow events of varying magnitude on ephemeral channels in a semiarid region. Geomorphology, the Natural and Human Structuring of Rivers and other Geomorphic Systems: a special issue in Honor of William L. Graf 252, 128–143. https://doi.org/10.1016/j.geomorph.2015.07.014.

Horacio, J., Ollero, A., Pérez-Alberti, A., 2017. Geomorphic classification of rivers: a new methodology applied in an Atlantic Region (Galicia, NW Iberian Peninsula). Environ. Earth Sci. 76, 746. https://doi.org/10.1007/s12665-017-7072-0.

Knighton, A.D., 1999. Downstream variation in stream power. Geomorphology 29, 293–306. https://doi.org/10.1016/S0169-555X(99)00015-X.

Kondolf, G.M., 1997. PROFILE: Hungry Water: Effects of Dams and Gravel Mining on River Channels. Environ. Manag. 21, 533–551. https://doi.org/10.1007/s002679900048.

Kondolf, G.M., Boulton, A.J., O'Daniel, S., Poole, G.C., Rahel, F.J., Stanley, E.H., Wohl, E., Bång, A., Carlstrom, J., Cristoni, C., Huber, H., Koljonen, S., Louhi, P., Nakamura, K., 2006. Process-based Ecological River Restoration: Visualizing Three-Dimensional Connectivity and Dynamic Vectors to Recover lost Linkages. Ecol. Soc. 11.

Kuhn, M., 2020. caret: Classification and Regression Training.

Lekach, J., Enzel, Y., 2021. Flood-duration-integrated stream power and frequency magnitude of >50-year-long sediment discharge out of a hyperarid watershed. Earth Surf. Process. Landf. 46, 1348–1362. https://doi.org/10.1002/esp.5104.

Martínez-Fernández, V., Solana-Gutiérrez, J., González del Tánago, M., García de Jalón, D., 2016. Automatic procedures for river reach delineation: Univariate and multivariate approaches in a fluvial context. Geomorphology 253, 38–47. https://doi.org/10.1016/j.geomorph.2015.09.029.

Martínez-Fernández, V., González del Tánago, M., García de Jalón, D., 2019. Selecting geomorphic variables for automatic river segmentation: Trade-offs between information gained and effort required. Geomorphology 329, 248–258. https://doi.org/10.1016/j.geomorph.2019.01.005.

McFeeters, S.K., 1996. The use of the Normalized Difference Water Index (NDWI) in the delineation of open water features. Int. J. Remote Sens. 17, 1425–1432. https://doi.org/10.1080/01431169608948714.

Mielke, P.W., 1991. The application of multivariate permutation methods based on distance functions in the earth sciences. Earth Sci. Rev. 31, 55–71. https://doi.org/10.1016/0012-8252(91)90042-E.

Mould, S., Fryirs, K., 2018. Contextualising the trajectory of geomorphic river recovery with environmental history to support river management. Applied Geography 94, 130–146. https://doi.org/10.1016/j.apgeog.2018.03.008.

Newson, Malcolm D., Large, A.R.G., 2006. 'Natural' rivers, 'hydromorphological quality' and river restoration: a challenging new agenda for applied fluvial geomorphology. Earth Surf. Process. Landf. 31, 1606–1624. https://doi.org/10.1002/esp.1430.

Ollero, A., Conesa, C., Vidal-Abarca, M.R., 2022. A Guide to Good Practices for the Management and Restoration of Mediterranean Ephemeral Streams: Resilence and Adaptation to Climate Change. Ediciones de la Universidad de Murcia.

Phiri, D., Simwanda, M., Salekin, S., Nyirenda, V.R., Murayama, Y., Ranagalage, M., 2020. Sentinel-2 Data for Land Cover/Use Mapping: a Review. Remote Sens. (Basel) 12, 2291. https://doi.org/10.3390/rs12142291.

Picco, L., Pellegrini, G., Iroumé, A., Lenzi, M.A., Rainato, R., 2023. The role of in-channel vegetation in driving and controlling the geomorphic changes along a gravel-bed river. Geomorphology 437, 108803. https://doi.org/10.1016/j.geomorph.2023.108803.

Piégay, H., Mathias Kondolf, G., Sear, D.A., 2016. Integrating geomorphological tools to address practical problems in river management and restoration. Tools in Fluvial Geomorphology. 507–532. https://doi.org/10.1002/9781118648551.ch22.

R Core Team, 2022. R: A Language and Environment for Statistical Computing. R Foundation for Statistical Computing, Vienna, Austria.

Rabanaque, M.P., Martínez-Fernández, V., Benito, G., 2021. Caracterización diacrónica de formas y cambios fluviales mediante análisis automatizado de ortofotografías y técnicas de machine learning. Cuadernos de Geografía de la Universitat de València 49–68. https://doi.org/10.7203/CGUV.107.21218.

Rabanaque, M.P., Martínez-Fernández, V., Calle, M., Benito, G., 2022. Basin-wide hydromorphological analysis of ephemeral streams using machine learning algorithms. Earth Surf. Process. Landf. 47, 328–344. https://doi.org/10.1002/esp.5250.

Rinaldi, M., 2003. Recent channel adjustments in alluvial rivers of Tuscany, Central Italy. Earth Surf. Process. Landf. 28, 587–608. https://doi.org/10.1002/esp.464.

Rinaldi, M., Gurnell, A.M., del Tánago, M.G., Bussettini, M., Hendriks, D., 2016. Classification of river morphology and hydrology to support management and restoration. Aquat. Sci. 78, 17–33. https://doi.org/10.1007/s00027-015-0438-z.

Rodriguez-Lloveras, X., Buytaert, W., Benito, G., 2016. Land use can offset climate change induced increases in erosion in Mediterranean watersheds. CATENA 143, 244–255. https://doi.org/10.1016/j.catena.2016.04.012.

Rouse, J.W., Haas, R.H., Schell, J.A., Deering, D.W., 1974. Monitoring vegetation systems in the Great Plains with ERTS. NASA Special Publication 351, 309–317.

Roux, C., Alber, A., Bertrand, M., Vaudor, L., Piégay, H., 2015. "FluvialCorridor": a new ArcGIS toolbox package for multiscale riverscape exploration. Geomorphology, Geomorphology in the Geocomputing Landscape: GIS, DEMs, Spatial Analysis and statistics 242, 29–37. https://doi.org/10.1016/j.geomorph.2014.04.018.

Sanchis-Ibor, C., Segura-Beltrán, F., 2014. Spatial variability of channel changes in a Mediterranean ephemeral stream in the last six decades (1946-2006). Cuadernos de Investigación Geográfica 40, 89. https://doi.org/10.18172/cig.2530.

Sanchis-Ibor, C., Segura-Beltrán, F., Almonacid-Caballer, J., 2017. Channel forms recovery in an ephemeral river after gravel mining (Palancia River, Eastern Spain). Catena 158, 357–370. https://doi.org/10.1016/j.catena.2017.07.012.

Scamardo, J., Nichols, M., Rittenour, T., Wohl, E., 2023. Drivers of Geomorphic Heterogeneity in Unconfined Non-Perennial River Corridors. J. Geophys. Res. Earth 128, e2023JF007102. https://doi.org/10.1029/2023JF007102.

Segura-Beltrán, F., Sanchis-Ibor, C., 2013. Assessment of channel changes in a Mediterranean ephemeral stream since the early twentieth century. The Rambla de Cervera, eastern Spain. Geomorphology 201, 199–214. https://doi.org/10.1016/j.geomorph.2013.06.021.

Segura-Beltrán, F., Sanchis-Ibor, C., Vidal-Salvador, A., 2020. La incisión como efecto de los cambios ambientales en ríos efímeros, in: Desafíos y Oportunidades de Un Mundo En Transición: Una Interpretación Desde La Geografía. PUV-Tirant lo Blanch, pp. 145–160.

Simón, J.L., Pérez-Cueva, A.J., Calvo-Cases, A., 2013. Tectonic beheading of fluvial valleys in the Maestrat grabens (eastern Spain): Insights into slip rates of Pleistocene extensional faults. Tectonophysics 593, 73–84. https://doi.org/10.1016/j.tecto.2013.02.026.

Stubbington, R., Paillex, A., England, J., Barthès, A., Bouchez, A., Rimet, F., Sánchez-Montoya, M.M., Westwood, C.G., Datry, T., 2019. A comparison of biotic groups as dry-phase indicators of ecological quality in intermittent rivers and ephemeral streams. Ecol. Indic. 97, 165–174. https://doi.org/10.1016/j.ecolind.2018.09.061.

Suárez, M.L., Vidal-Abarca, M.R., 2008. Índice para valorar el estado de conservación de las ramblas mediterráneas (índice de alteración de ramblas o IAR). Tecnología del agua 293, 67–78.

Thanh Noi, P., Kappas, M., 2018. Comparison of Random Forest, k-Nearest Neighbor, and support Vector Machine Classifiers for Land Cover Classification using Sentinel-2 Imagery. Sensors 18, 18. https://doi.org/10.3390/s18010018.

Wohl, E., Merritts, D.J., 2007. What is a Natural River? Geogr. Compass 1, 871–900. https://doi.org/10.1111/j.1749-8198.2007.00049.x.